

A low-dimensional analogue of holographic baryons

Stefano Bolognesi and Paul Sutcliffe

Department of Mathematical Sciences, Durham University, Durham DH1 3LE, U.K.

Email: s.bolognesi@durham.ac.uk & p.m.sutcliffe@durham.ac.uk

November 2013

Abstract

Baryons in holographic QCD correspond to topological solitons in the bulk. The most prominent example is the Sakai-Sugimoto model, where the bulk soliton in the five-dimensional spacetime of AdS-type can be approximated by the flat space self-dual Yang-Mills instanton with a small size. Recently, the validity of this approximation has been verified by comparison with the numerical field theory solution. However, multi-solitons and solitons with finite density are currently beyond numerical field theory computations. Various approximations have been applied to investigate these important issues and have led to proposals for finite density configurations that include dyonic salt and baryonic popcorn. Here we introduce and investigate a low-dimensional analogue of the Sakai-Sugimoto model, in which the bulk soliton can be approximated by a flat space sigma model instanton. The bulk theory is a baby Skyrme model in a three-dimensional spacetime with negative curvature. The advantage of the lower-dimensional theory is that numerical simulations of multi-solitons and finite density solutions can be performed and compared with flat space instanton approximations. In particular, analogues of dyonic salt and baryonic popcorn configurations are found and analysed.

1 Introduction

A common feature of all models of holographic QCD is that baryons correspond to topological solitons in the bulk. The foremost example of a top-down theory with a string theory embedding is the Sakai-Sugimoto model [1, 2], which results in a Yang-Mills theory with a Chern-Simons term in a five-dimensional bulk spacetime of AdS-type. As there is an identification between baryon number and instanton charge, the study of baryons is equivalent to the construction of Yang-Mills-Chern-Simons solitons in curved space, with a prescribed instanton number.

At large 't Hooft coupling the Yang-Mills term dominates over the Chern-Simons term and the soliton has a small size, determined by balancing curvature and Chern-Simons contributions to the action. As the soliton is small compared to the curvature scale then it can be approximated by a flat space self-dual Yang-Mills instanton with a small size [3, 4]. The validity of this approximation has recently been confirmed by numerical field theory computations [5], by exploiting the $SO(3)$ symmetry of the static single soliton to reduce the computation in four-dimensional space to a reduced theory in a two-dimensional space. However, multi-solitons (including solitons at finite density) are unlikely to have any continuous symmetries, so numerical field theory computations would require a fully four-dimensional computation that is beyond current capabilities.

The construction of solitons at finite density is a crucial aspect for understanding the important issue of dense QCD. In the limit of a large number of colours, which is the regime of holographic QCD, cold nuclear matter becomes a crystalline solid, although the details of this are still to be understood. It should be possible to capture this behaviour via a bulk soliton description within holographic QCD and in particular within the Sakai-Sugimoto model. However, the lack of numerical computations has led to various approximate methods being employed to describe this phase, as follows.

Calorons, which are flat space self-dual Yang-Mills instantons with a periodic direction, can split into monopole constituents if the period is smaller than the instanton size. This fact, together with a point particle approximation, has led to the suggestion [6] that the appropriate soliton crystal consists of pairs of dyons with opposite charges arranged in a salt-like configuration. It is argued that, with increasing density, this dyonic salt arrangement turns into a cubic crystal of half-instantons that is dual to the well-known Skyrme crystal. In a different study, making use of approximations involving flat space calorons and dilute instantons, it has been proposed [7, 8] that with increasing density a series of transitions takes place, dubbed baryonic popcorn, where the three-dimensional soliton crystal develops additional layers in the holographic direction. Unfortunately, field theory computations are not yet available to test these ideas in the Sakai-Sugimoto model.

In this paper we introduce and investigate a low-dimensional analogue of the Sakai-Sugimoto model. The bulk theory is defined in a three-dimensional spacetime with negative curvature, and is an $O(3)$ sigma model with a baby Skyrme term that plays the role of the Chern-Simons term in the higher dimensional theory. It is well-known that instantons in planar sigma models are natural low-dimensional analogues of Yang-Mills instantons. If the coefficient of the baby Skyrme term is small then the soliton has a small size and may be

approximated by an instanton of the flat space sigma model. The advantage of the lower-dimensional theory is that numerical simulations of multi-solitons and finite density solutions can be performed and compared with predictions using flat space instanton approximations. In particular, analogues of dyonic salt and baryonic popcorn configurations are found and analysed. The results provide evidence to support the validity of these ideas within the Sakai-Sugimoto model.

2 Solitons of a holographic baby Skyrme model

Consider a $(D + 2)$ -dimensional spacetime with a metric of the form

$$ds^2 = H(-dt^2 + dx_1^2 + \dots + dx_D^2) + \frac{1}{H}dz^2, \quad (2.1)$$

where

$$H(z) = \left(1 + \frac{z^2}{L^2}\right)^p. \quad (2.2)$$

The warp factor $H(z)$, multiplying the $(D + 1)$ -dimensional Minkowski spacetime of the dual boundary theory, depends only on the additional holographic coordinate z . The constant p is to be specified later and L determines the curvature length scale and can be set to unity by an appropriate choice of units.

The metric of the Sakai-Sugimoto model [1, 2] corresponds to the choice $D = 3$ and $p = \frac{2}{3}$. In this case the spacetime has a conformal boundary as $z \rightarrow \infty$ and the scalar curvature is

$$R = -\frac{16(4z^2 + 3)}{9(1 + z^2)^{4/3}}, \quad (2.3)$$

with the properties that $R \leq 0$ and R is finite (in fact zero) as $z \rightarrow \infty$.

In this paper we are interested in a low-dimensional analogue with $D = 1$, so that the bulk spacetime is three-dimensional with coordinates t, x, z . In this case, for general p , the scalar curvature is

$$R = -2p(1 + z^2)^{p-2} \left((5p - 2)z^2 + 2 \right). \quad (2.4)$$

For this spacetime to have finite curvature with $R \leq 0$ requires the restriction $\frac{2}{5} \leq p \leq 1$. Later we shall see that a convenient choice is $p = \frac{1}{2}$, but for now we consider a general value of p within the above interval.

The action of the massless $O(3)$ baby Skyrme model in the above spacetime is

$$S = \int \left(\frac{1}{2} g^{\mu\nu} \partial_\mu \phi \cdot \partial_\nu \phi + \frac{\kappa^2}{4} g^{\mu\nu} g^{\alpha\beta} (\partial_\mu \phi \times \partial_\alpha \phi) \cdot (\partial_\nu \phi \times \partial_\beta \phi) \right) \sqrt{-g} dx dz dt, \quad (2.5)$$

where $\phi = (\phi_1, \phi_2, \phi_3)$ is a three-component unit vector and greek indices run over the bulk spacetime components t, x, z . The first term in (2.5) is that of the $O(3)$ sigma model and the second term, with constant coefficient κ^2 , is the baby Skyrme term [9].

The associated static energy is

$$E = \frac{1}{2} \int \left(\frac{1}{H} |\partial_x \phi|^2 + H |\partial_z \phi|^2 + \kappa^2 |\partial_x \phi \times \partial_z \phi|^2 \right) \sqrt{H} dx dz, \quad (2.6)$$

and the boundary condition is that $\phi \rightarrow (0, 0, 1)$ as $x^2 + z^2 \rightarrow \infty$. As we shall see, this theory has bulk topological solitons that share many analogous features to those in the Sakai-Sugimoto model. The analogue of the baryon number is the integer-valued topological charge

$$B = -\frac{1}{4\pi} \int \phi \cdot (\partial_x \phi \times \partial_z \phi) dx dz, \quad (2.7)$$

which defines the instanton number of the planar sigma model.

Using the fact that the baby Skyrme term contribution to the energy is non-negative and $H \geq 1$, together with the obvious inequality

$$\left| \frac{1}{\sqrt{H}} \partial_x \phi \pm \sqrt{H} \phi \times \partial_z \phi \right|^2 \geq 0, \quad (2.8)$$

yields the Bogomolny bound $E \geq 4\pi|B|$.

In flat space ($H = 1$) without a baby Skyrme term ($\kappa = 0$) this inequality is attained by the instanton solutions of the $O(3)$ sigma model (for a review see [10]). To write these instanton solutions explicitly it is convenient to use the equivalent formulation of the $O(3)$ sigma model in terms of the \mathbb{CP}^1 sigma model. This is obtained by defining the Riemann sphere coordinate $W = (\phi_1 + i\phi_2)/(1 - \phi_3)$, obtained by stereographic projection of ϕ . In terms of this variable, instanton solutions are given by W a holomorphic function of $\zeta = x + iz$. The instanton solutions with finite $B > 0$ are given by $W(\zeta)$ a rational function of degree B , where the degree of the numerator is larger than that of the denominator in order to satisfy the above boundary condition. Taking into account the global $U(1)$ symmetry associated with the phase of W , this leaves an instanton moduli space \mathcal{M}_B of dimension $4B - 1$.

The radially symmetric sigma model instanton with topological charge B and centre at the origin is given by $W = (\zeta/\mu)^B$, where the positive real constant μ is the arbitrary size of the instanton. Converting back to the $O(3)$ sigma model formulation this solution is

$$\phi = (\sin f \cos(B\theta), \sin f \sin(B\theta), \cos f), \quad (2.9)$$

where r, θ are polar coordinates in the (x, z) -plane and $f(r)$ is the radial profile function

$$f = \cos^{-1} \left(\frac{r^{2B} - \mu^{2B}}{r^{2B} + \mu^{2B}} \right). \quad (2.10)$$

If we require that this field configuration has finite energy in the curved spacetime theory (2.6) then this places a further restriction on the power p , as follows. The large r behaviour of the profile function is

$$f = \frac{2\mu^B}{r^B} + \dots \quad (2.11)$$

so the greatest restriction arises when $B = 1$. Convergence of the energy requires that $p < 2/3$, which combined with the earlier restriction yields $\frac{2}{5} \leq p < \frac{2}{3}$. The choice of p is therefore quite restricted and $p = \frac{1}{2}$ is a natural value to take and will be used in all our numerical computations. However, we shall often leave p general in our analytic calculations, to make it clear which terms derive directly from the curvature of the metric, though it is to be understood that any formulae are only to be applied with p in the above restricted range.

To make our analogy with the Sakai-Sugimoto model, we consider a regime in which $0 < \kappa \ll 1$; this being the analogue of large 't Hooft coupling. In this regime the sigma model term dominates over the baby Skyrme term and it is reasonable to approximate the soliton by a sigma model instanton. In flat space the static sigma model is conformally invariant and therefore an instanton has an arbitrary size. However, in the above spacetime the curvature breaks this energy degeneracy of the sigma model and without a baby Skyrme term the static energy is a monotonically decreasing function of the instanton size. The inclusion of the baby Skyrme term produces a contribution to the energy that increases with decreasing instanton size and balances the curvature contribution to yield a preferred non-zero instanton size; though it is small because the coefficient of the baby Skyrme term is small. Below we make this qualitative analysis more concrete through explicit calculation.

To extract the sigma model instanton, that arises in the small κ limit, we define the rescaled variables $\tilde{x} = x/\sqrt{\kappa}$ and $\tilde{z} = z/\sqrt{\kappa}$, with \tilde{H} denoting $H(\tilde{z}\sqrt{\kappa})$. In terms of these variables the energy (2.6) becomes

$$E = \frac{1}{2} \int \left(\tilde{H}^{-1/2} |\partial_{\tilde{x}} \phi|^2 + \tilde{H}^{3/2} |\partial_{\tilde{z}} \phi|^2 + \kappa \tilde{H}^{1/2} |\partial_{\tilde{x}} \phi \times \partial_{\tilde{z}} \phi|^2 \right) d\tilde{x} d\tilde{z}. \quad (2.12)$$

Expanding this energy as a series in κ yields $E = E_0 + \kappa E_1 + \mathcal{O}(\kappa^2)$, where

$$E_0 = \frac{1}{2} \int \left(|\partial_{\tilde{x}} \phi|^2 + |\partial_{\tilde{z}} \phi|^2 \right) d\tilde{x} d\tilde{z}, \quad (2.13)$$

$$E_1 = \int \left(\frac{1}{4} p \tilde{z}^2 (3 |\partial_{\tilde{z}} \phi|^2 - |\partial_{\tilde{x}} \phi|^2) + \frac{1}{2} |\partial_{\tilde{x}} \phi \times \partial_{\tilde{z}} \phi|^2 \right) d\tilde{x} d\tilde{z}. \quad (2.14)$$

The static energy (2.13) is that of the planar flat space $O(3)$ sigma model, in rescaled variables, and is minimized by the instanton solutions with $E_0 = 4\pi B$. This motivates the approximation of restricting the field to an instanton configuration and then determining the point in the instanton moduli space, \mathcal{M}_B , that minimizes the energy (2.12). To make analytic progress, a further approximation can be employed by neglecting terms in the energy beyond linear order in κ , that is, $E \approx 4\pi B + \kappa E_1$. With this additional approximation E_1 becomes an energy function on \mathcal{M}_B , and the task reduces to finding its minimum.

As an illustration of this procedure we first consider a subset of \mathcal{M}_B given by restricting to radially symmetric instantons $W = (\zeta/\mu)^B$, with scale μ . The curvature in the holographic direction acts as an effective potential with a minimum at $z = 0$ and as the energy is invariant under translations in the x direction then there is no loss of generality in positioning the radial instanton at the origin. In terms of the rescaled variables $\tilde{\zeta} = \zeta/\sqrt{\kappa}$ and $\tilde{\mu} = \mu/\sqrt{\kappa}$

we have $W = (\tilde{\zeta}/\tilde{\mu})^B$, and for simplicity we first discuss the example with $B = 2$. In this case a simple calculation produces the result

$$E_1 = \pi^2 \left(p\tilde{\mu}^2 + \frac{4}{\tilde{\mu}^2} \right). \quad (2.15)$$

The influence of the curvature is evident in the term proportional to p in (2.15) and drives the instanton towards zero size. The second term in (2.15) originates from the baby Skyrme term and resists the shrinking of the instanton size. These competing effects combine to produce the finite size $\tilde{\mu} = \sqrt{2}/p^{1/4}$ that minimizes the energy (2.15). Returning to the original variables the size is $\mu = \sqrt{2\kappa}/p^{1/4}$ and is therefore small in the regime of small κ . The energy is dominated by the flat space instanton contribution 8π , as the correction from the size stabilizing terms is subleading, being linear in κ .

A similar calculation can be performed for all $B \geq 2$ to show that the instanton size is proportional to $\sqrt{\kappa}$. However, the corresponding analytic calculation for $B = 1$ is more difficult because E_1 is divergent in this case. The instanton approximation $W = \zeta/\mu$ is still valid but the series expansion of the energy in terms of κ is not. This is due to the fact that the first order correction involves approximating $H(z)$ by a quadratic in z , which is too crude an approximation for the slow decay of the $B = 1$ instanton. One approach is to use a more complicated approximation for $H(z)$ that captures the correct behaviour to quadratic order but matches better the large z behaviour of $H(z)$, so that all integrals are finite. However, this approach is cumbersome and an alternative method is to numerically compute the energy (2.6) of the ansatz $W = \zeta/\mu$ to determine the minimizing size μ as a function of κ . The result, for $p = \frac{1}{2}$, is displayed in Figure 1 for $\kappa \in [10^{-4}, 10^{-2}]$, where the data points correspond to the numerical computation and the curve is a fit to the data of the form $c\sqrt{\kappa}$ with the constant $c = 0.96$. This computation suggests that, in this regime, the $B = 1$ soliton has an approximate size $\sqrt{\kappa}$, in agreement with the above analytic computation for $B = 2$ that gives a size that is also $\mathcal{O}(\sqrt{\kappa})$.

The main advantage of our low-dimensional model is that we are able to obtain full numerical solutions of the nonlinear field theory, because the static problem is only two-dimensional and is therefore within the reach of modest computational resources. All our computations are performed for the model with $p = \frac{1}{2}$ and the parameter value $\kappa = 0.01$, so that the soliton has a size that is smaller than the curvature length scale. Other smaller values of κ have also been investigated and the results are similar. To numerically compute static solitons we minimize the energy (2.6) using second order accurate finite difference approximations for the spatial derivatives using lattice spacings $\Delta x = \Delta z = 0.005$ and numerical grids that contain 2000×2000 points. The energy minimization algorithm is an adaptation of the one described in detail in [11], where it is applied to the three-dimensional Skyrme model in flat space.

The result of our field theory computation for the $B = 1$ soliton is displayed in the left image in Figure 2, where we plot ϕ_3 , as this gives a good pictorial representation of the soliton. It can be seen that the soliton has an approximate radial symmetry and a size that is roughly $\sqrt{\kappa} = 0.1$, as predicted by the instanton approximation. In fact, a plot of ϕ_3 using the instanton approximation $W = \zeta/\mu$ with a size $\mu = 0.96\sqrt{\kappa}$ produces an indistinguishable

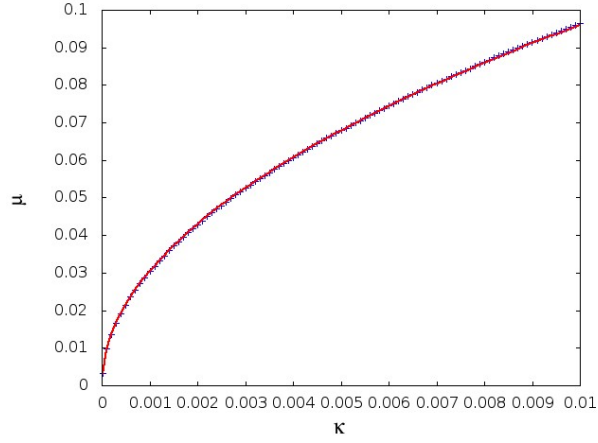


Figure 1: The data points give the size μ of the $B = 1$ soliton as a function of κ , within the instanton approximation. The curve is a numerical fit to the data of the form $c\sqrt{\kappa}$ with the constant $c = 0.96$.

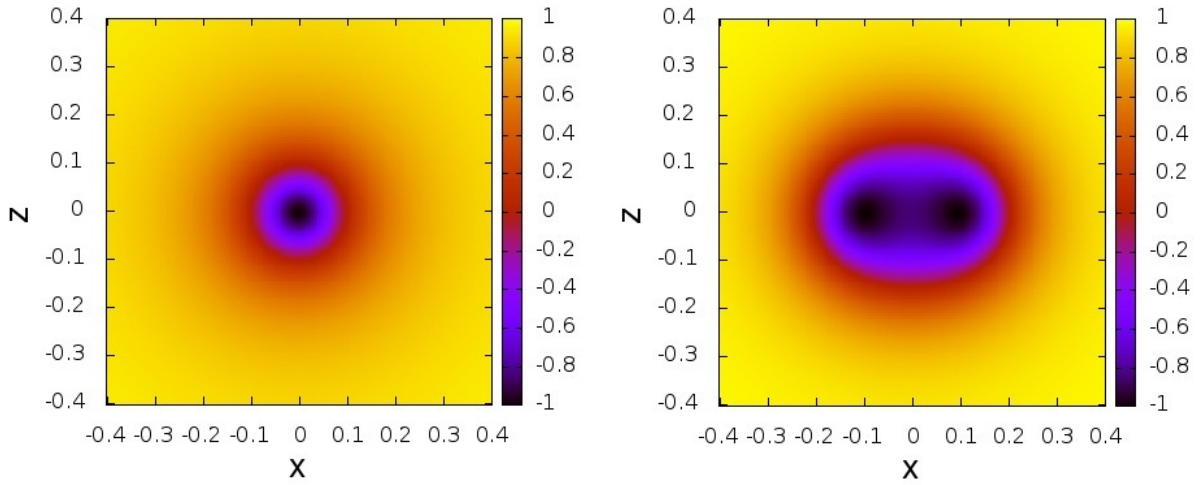


Figure 2: A plot of ϕ_3 for the soliton with $B = 1$ (left image) and $B = 2$ (right image).

image. The accuracy of the instanton approximation is confirmed by an energy comparison, as the numerical field theory computation yields a value $E = 4\pi \times 1.0148$ to be compared with the energy of the instanton approximation $E = 4\pi \times 1.0154$.

The right image in Figure 2 displays the result of the field theory computation for the $B = 2$ soliton. The energy is $E = 8\pi \times 1.0105$, so this is a bound state of two single solitons. Note that the binding energy per soliton is less than 0.5% of the single soliton energy, illustrating the fact that holographic models based on perturbations around BPS systems can yield the kind of small binding energies found in real nuclei. The $B = 2$ soliton does not have (even approximate) radial symmetry but resembles two single solitons separated along the non-holographic direction, with a separation that is close to the diameter of a single soliton. Below we present an analytic calculation that explains this result by making use of the 2-instanton moduli space \mathcal{M}_2 .

We investigate the $B = 2$ soliton by considering a two-dimensional subset of \mathcal{M}_2 that includes radial instantons. Explicitly, we consider instanton solutions of the form

$$W = \frac{\zeta^2 - a^2}{\mu^2}, \quad (2.16)$$

where μ and a are real parameters. This describes two instantons separated along the non-holographic direction with positions $(x, z) = (\pm a, 0)$ and μ determines their equal size. Radial solutions correspond to the choice $a = 0$. The idea is to determine, for each a , the size μ that minimizes the energy (2.6) and then show that as a function of a this energy has a minimum at a value of a that is $\mathcal{O}(\sqrt{\kappa})$. For any given value of κ this calculation can be performed by numerical integration of the energy (2.6). As an example, for $\kappa = 0.01$ and $p = \frac{1}{2}$ the black curve in Figure 3 displays $E/(8\pi)$ as a function of a , which clearly has a minimum at $a \approx 0.1 = \sqrt{\kappa}$.

To make analytic progress we perform the same rescaling introduced earlier, writing $\tilde{\mu} = \mu/\sqrt{\kappa}$ and $\tilde{a} = a/\sqrt{\kappa}$, and evaluate the first order correction to the energy E_1 . The resulting integrals can be evaluated by expanding around the radial case $\tilde{a} = 0$ to extend the result (2.15). To quartic order in \tilde{a}

$$E_1 = p \left(\pi^2 \tilde{\mu}^2 - 2\pi \tilde{a}^2 + \frac{\pi^2 \tilde{a}^4}{\tilde{\mu}^2} \right) + \frac{4\pi^2}{\tilde{\mu}^2} + \frac{5\pi^2 \tilde{a}^4}{\tilde{\mu}^6}, \quad (2.17)$$

so the minimizing size is

$$\tilde{\mu} = \frac{\sqrt{2}}{p^{1/4}} + \frac{1}{2^{3/2}} p^{3/4} \tilde{a}^4. \quad (2.18)$$

Substituting this size into (2.17) produces

$$E_1 = 4\pi^2 \sqrt{p} - 2\pi p \tilde{a}^2 + \frac{3}{4} \pi^2 p^{3/2} \tilde{a}^4, \quad (2.19)$$

hence the radial instanton is unstable to a perturbation that separates the two instantons along the non-holographic direction. Approximating the energy by neglecting quadratic and

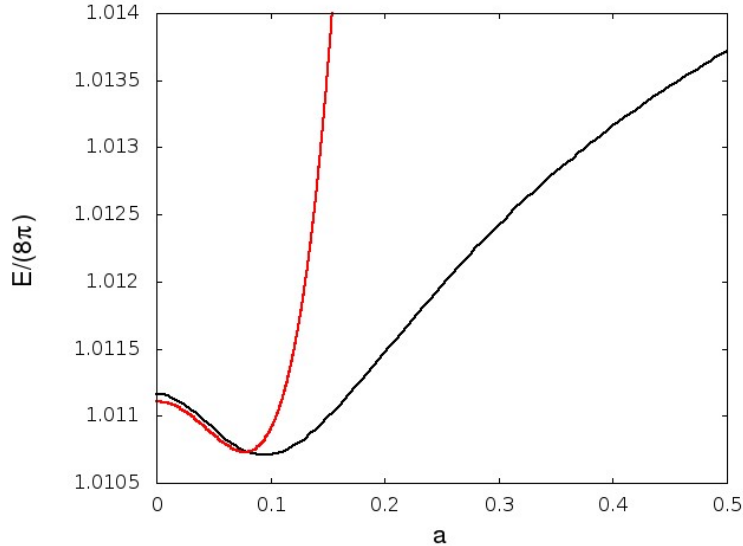


Figure 3: A plot of $E/(8\pi)$ for a 2-instanton configuration with separation $2a$ between the two instantons. The black curve is the result of a numerical integration to compute the energy and the red curve is the analytic approximation described in the text.

higher order terms in κ , that is $E \approx E_0 + \kappa E_1$, and returning to unscaled variables, the above result yields

$$\frac{E}{8\pi} \approx 1 + \frac{\pi}{2}\sqrt{p}\kappa - \frac{1}{4}pa^2 + \frac{3\pi}{32\kappa}p^{3/2}a^4. \quad (2.20)$$

This energy is minimized at the value

$$a = \frac{2}{p^{1/4}}\sqrt{\frac{\kappa}{3\pi}}, \quad (2.21)$$

so the required $\mathcal{O}(\sqrt{\kappa})$ dependence has indeed been obtained. Furthermore, this calculation reveals that the separation $2a$ between the two instantons is approximately equal to the size μ of the 2-instanton. In other words, it predicts that the 2-soliton solution should closely resemble two touching single solitons.

To test the accuracy of this approximation we can compare the formula (2.20) to the earlier numerical computation (black curve in Figure 3) with $\kappa = 0.01$ and $p = \frac{1}{2}$. For these parameter values the approximation (2.20) is shown as the red curve in Figure 3. This shows that the qualitative features are correct and that the approximation is reasonably accurate for separations up to the minimizing value, and in particular the estimate for the energy minimizing separation is reasonable.

From the numerical data used to produce the black curve in Figure 3, it is found that the energy is minimized for the instanton parameters $a = 0.095$ and $\mu = 0.18$ with an energy that is only 0.03% above the field theory computation. As expected from this result, a plot

of ϕ_3 using this instanton approximation produces an image that is essentially identical to the right image displayed in Figure 2.

We have also computed solitons with larger values of B . The result yields a string of B single solitons that are touching and aligned along the non-holographic direction, as expected given the above result for $B = 2$ and the fact that the curvature favours solitons located along the line $z = 0$. In the following section we turn our attention to solitons with finite density and display some interesting phenomena.

3 Solitons at finite density

As mentioned in the introduction, the study of solitons at finite density in the Sakai-Sugimoto model has attracted some recent attention in attempts to understand dense QCD within a holographic setting. However, various levels of approximation have to be made to make any progress on this topic, given that numerical field theory simulations are currently not available. Furthermore, even the relevant flat space self-dual instanton solutions are not explicitly known once periodic boundary conditions are applied in multiple directions, which is precisely the case of interest. However, in our low-dimensional analogue not only are we able to compute the numerical field theory solutions, but we also have access to simple explicit formulae for the relevant periodic flat space instantons. This allows us to investigate solitons with finite density using both approaches and to compare the results. In particular, we find analogues of the phenomena suggested for the Sakai-Sugimoto model and are able to study these in some detail.

To numerically compute solitons at finite density we restrict our numerical grid in the non-holographic direction to the range $-L \leq x \leq L$ and impose periodic boundary conditions by identification of the fields at $x = \pm L$. The integral expression (2.7) for the baryon number, with the range of integration now restricted to the strip $(x, z) \in [-L, L] \times (-\infty, \infty)$, is still integer-valued and defines the finite density $\rho = B/(2L)$. Initial conditions are obtained by using the radial field (2.9) with $B = 1$ and a profile function $f(r)$ with compact support so that $f(0) = \pi$ and $f(r) = 0$ for $r \geq r_*$, for a suitably chosen constant r_* . A periodic field with topological charge B can then be created by a linear superposition of B fields of this form, where the position of each soliton is shifted so that the separation between any pair of solitons is greater than $2r_*$. In this construction of the initial field configuration, each soliton can independently be given an arbitrary phase χ , corresponding to a shift $\theta \mapsto \theta + \chi$ in the radial field (2.9).

In fact, we already have evidence that the most attractive arrangement of two solitons is associated with a relative phase of π between the two solitons. This evidence follows from the following argument. In terms of the $\mathbb{C}P^1$ coordinate W , the product ansatz for two fields W_1 and W_2 is

$$W = \frac{W_1 W_2}{W_1 + W_2}. \quad (3.1)$$

This has the property that W is zero whenever W_1 or W_2 is zero, so there are solitons at the positions given by the two constituent components. Furthermore, in a region of space far

from the soliton described by one of the components, say W_2 , then this component is large so $W \approx W_1$, and vice-versa. Consider the above product for two solitons of equal size, with a relative phase χ and positions $\pm a$ along the x -axis. Explicitly,

$$W_1 = \frac{\zeta - a}{\nu}, \quad W_2 = e^{i\chi} \frac{\zeta + a}{\nu}, \quad \text{producing} \quad W = \frac{e^{i\chi}(\zeta^2 - a^2)}{\nu(\zeta(e^{i\chi} + 1) + a(e^{i\chi} - 1))}. \quad (3.2)$$

For the above field to match the expression (2.16), that is a good description of the minimal energy $B = 2$ soliton, requires $e^{i\chi} = -1$ and $\nu = \mu^2/(2a)$. Thus to have the two solitons in the most attractive channel requires the relative phase to be π , that is neighbouring solitons should be exactly out of phase.

The above argument is confirmed by our numerical simulations at finite density, where it is found that a chain of solitons which are all in phase has a higher energy per soliton than a chain in which the phase of the solitons alternates between 0 and π . Note that in the case of alternating phases the number of solitons in the chain in a fundamental period must be even to have a strictly periodic field. Under translation by the inter-soliton separation the field is only periodic up to a change of sign.

To calculate the energy per soliton E/B as a function of the density $\rho = B/(2L)$ for a single chain of solitons with alternating phases, we perform computations for a range of grid sizes $2L$, using an initial configuration with $B = 4$, so that the simulation region contains two fundamental periods. The optimal density is found to be $\rho = 2.8$, at which the energy per soliton is $E/B = 4\pi \times 1.0097$. The left image in Figure 4 displays ϕ_3 for this optimal density chain. In Figure 5 the data points marked with a + represent E/B , in units of 4π , for the numerical field theory solution of this chain. Note that the optimal density corresponds to the critical value of the chemical potential at which there is a first order phase transition to an equilibrium density of solitons, this being the analogue of the nuclear matter phase transition in QCD.

The chain solution at high density is displayed in the right image in Figure 4, which corresponds to the density $\rho = 10$, being more than three times the optimal density. At such a high density each soliton splits into a kink anti-kink pair separated along the holographic direction, and the solitons lose their individual identities to form an almost homogeneous structure in the non-holographic direction. This is the lower-dimensional analogue of the appearance of monopole constituents for calorons and has been discussed previously for instantons of the $O(3)$ sigma model in flat space [12, 13, 14]. A configuration of this type is therefore our low-dimensional analogue of the dyonic salt arrangement discussed in [6]. Furthermore, we can make use of the flat space sigma model results to study finite density configurations semi-analytically, as follows.

The starting point is the periodic sigma model solution considered in [12]

$$W = \nu \sin(\pi\rho\zeta), \quad (3.3)$$

that describes an instanton chain in which there are instantons located along the x -axis with a distance $1/\rho$ between neighbouring instantons (recall that the position of an instanton corresponds to a point where W vanishes). Note that this field obeys the symmetry relation

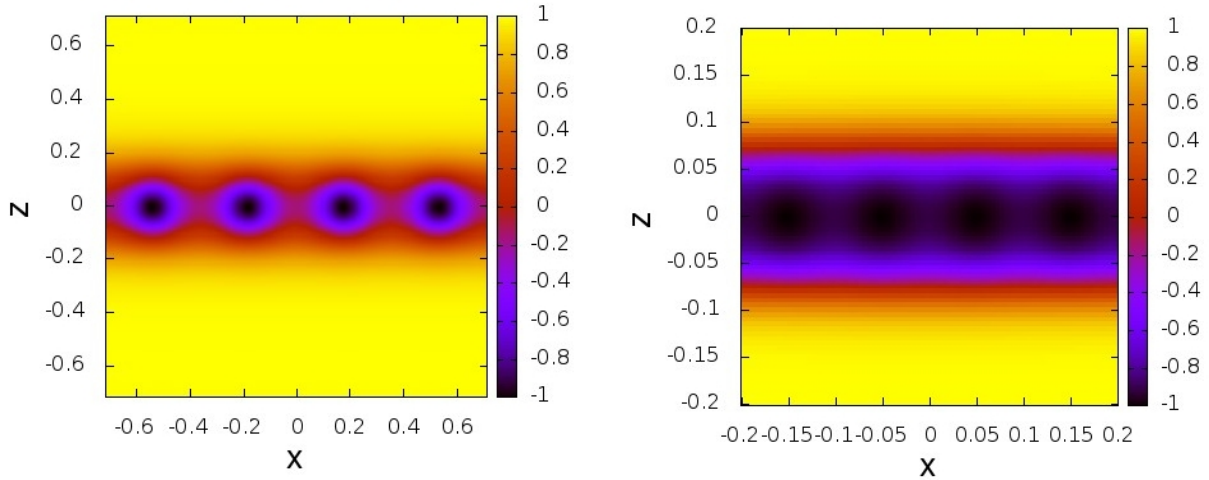


Figure 4: A plot of ϕ_3 for a chain with the optimal density $\rho = 2.8$ (left image) and the density $\rho = 10$ (right image).

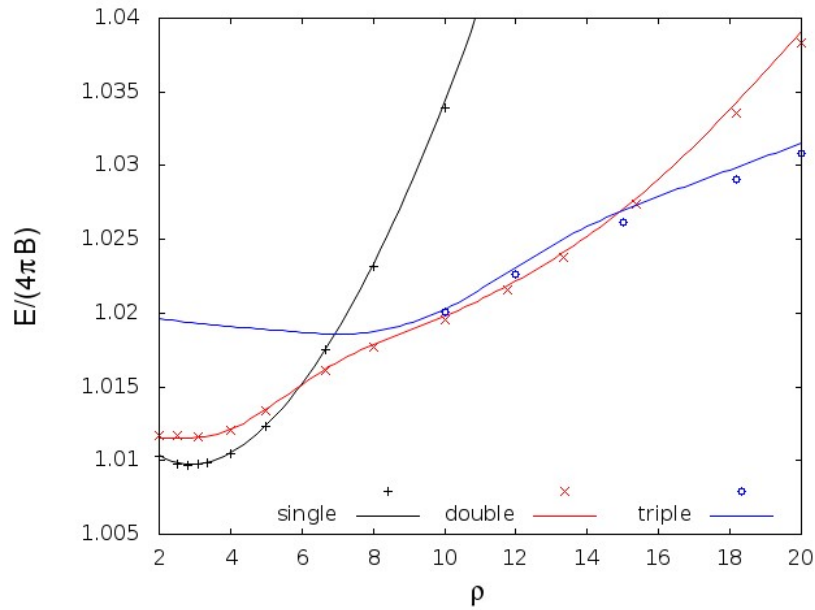


Figure 5: A plot of $E/(4\pi B)$ against density ρ for the single chain, double chain and triple chain configurations. Data points are the numerical solutions from field theory simulations and curves are sigma model instanton approximations.

$W(\zeta + \rho^{-1}) = -W(\zeta)$, which shows that neighbouring instantons are exactly out of phase, so this is a chain of instantons with alternating phases. The real parameter ν controls the size of each instanton, which is given by $1/(\nu\pi\rho)$ in the dilute regime where the instanton size is small compared to $1/\rho$. Once the instanton size is comparable to $1/\rho$ the instantons lose their individual identities and as the size increases further they split into kink anti-kink constituents and the configuration tends towards a homogeneous state [12, 13, 14].

The above instanton chain can be used to approximate the soliton chain of our holographic model. For any given density ρ , the energy (2.6) of the field (3.3) can be computed by numerical integration and a minimization performed over the parameter ν to determine the minimal energy. The result of such a computation is displayed as the black curve in Figure 5, where it can be seen that this instanton approximation is in excellent agreement with the data from field theory simulations. We have therefore shown, using two different approaches, how a chain of solitons splits into kink anti-kink constituents, in analogy to the proposed dyonic salt.

Beyond the optimal density, the energy per soliton of the chain grows rapidly with increasing density. The baryonic popcorn idea introduced in [7, 8] suggests that there will be a critical density beyond which it is energetically preferable for the soliton chain to split into a pair of chains via a pop into the holographic direction. To investigate this possibility we perform field theory simulations using initial conditions that describe a double chain. The result for the double chain with density $\rho = 10$ is displayed in the left image in Figure 6, where the phase of the solitons alternates within each chain. The two chains are aligned and two solitons in different chains with the same x coordinate are out of phase. This is the expected arrangement to allow maximal attraction between all neighbouring solitons and it can be confirmed that other possibilities, such as a relative shift between the two chains or a zig-zag arrangement, relax back to this solution under energy minimization. In Figure 5 the data points marked with a \times denote the energy per soliton (in units of 4π) as a function of the density for the double chain solution obtained from field theory simulations. These results show that the double chain solution has a lower energy than the single chain solution once the density is greater than about twice the optimal density.

As in the case of the single soliton chain, the double soliton chain can also be studied using an instanton approximation. The appropriate instanton can be obtained using the product ansatz (3.1) with constituent fields obtained by translation of the single chain form (3.3). Explicitly, take

$$W_1 = \nu \sin(\pi\rho(\zeta - i\delta)/2), \quad W_2 = -\nu \sin(\pi\rho(\zeta + i\delta)/2), \quad (3.4)$$

and minimize the energy over the scale ν and the distance 2δ between the chains in the holographic direction. The result is shown as the red curve in Figure 5 and is again in good agreement with the field theory computations. Both approaches therefore confirm the analogue of baryonic popcorn in our low-dimensional model. In particular, in the low-dimensional theory we find that the popcorn phenomenon takes place at a density below that at which the solitons split into constituents, so our popcorn is not salted.

In the study of baryonic popcorn in the Sakai-Sugimoto model it has been proposed that multiple chains have a zig-zag structure [7, 8]. A zig-zag structure requires that the optimal

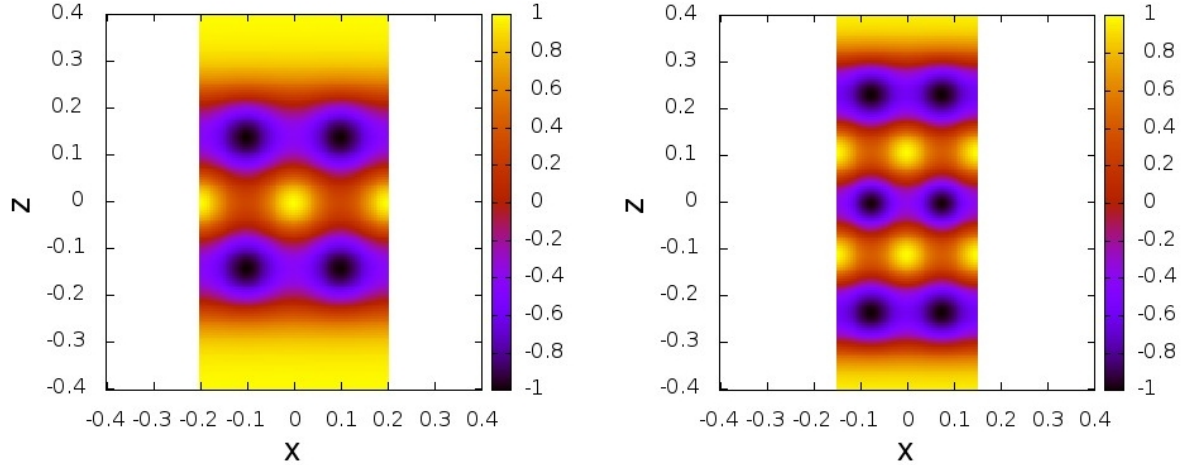


Figure 6: A plot of ϕ_3 for the double chain solution with density $\rho = 10$ (left image) and the triple chain solution with density $\rho = 20$ (right image).

separation for two solitons is much greater than the size of a single soliton. As this is not the case in our low-dimensional theory then it is not surprising that zig-zag solutions do not appear. The double chain instanton (3.4) can be modified to describe a zig-zag structure and this also supports the conclusion that it is not an energetically favourable configuration in this theory.

As one might expect, as the density is increased further the lowest energy configuration becomes a triple chain solution. An example field theory computation for the density $\rho = 20$ is shown in the right image in Figure 6. The energy per soliton (in units of 4π) for triple chain solutions computed from field theory simulations are shown in Figure 5 as the data points marked with a \circ for several densities. A triple chain instanton can be obtained by an obvious generalization of the double chain instanton (3.4). A minimization over the parameters in such an instanton approximation yields the blue curve in Figure 5, which agrees with the field theory results. These results confirm that a triple chain solution is energetically preferred over a double chain solution for sufficiently high density, as expected from the popcorn phenomenon. All these results suggest that as the density is increased further then the number of soliton chains increases and eventually the configuration begins to resemble a portion of a two-dimensional lattice rather than the one-dimensional chain that arises at the optimal density. This is exactly the phenomenon predicted in [7, 8].

4 Conclusion

In this paper we have introduced and investigated a holographic baby Skyrme model that can be used to study several low-dimensional analogues of bulk solitons in the Sakai-Sugimoto model, describing holographic baryons. The advantage of the low-dimensional theory is that

several aspects that one would like to study in the Sakai-Sugimoto model, but are currently not tractable, can be investigated exactly. In particular, we have compared sigma model instanton approximations with the results of field theory simulations and shown that this provides a good approximation for solitons, multi-solitons and finite density solutions. This provides further support for the use of self-dual Yang-Mills instantons in approximating bulk solitons in the Sakai-Sugimoto model. Analogues of dyonic salt and baryonic popcorn configurations have been found, providing strong evidence for their relevance in the study of holographic baryons.

We have used a baby Skyrme term to provide a low-dimensional analogue of the Chern-Simons term that appears in the Sakai-Sugimoto model. Perhaps a more obvious analogue of the Chern-Simons term is to couple a vector meson to the sigma model topological current, as studied in flat space in [15]. Note that the results in that paper show that this can produce similar results to the inclusion of a baby Skyrme term. As the baby Skyrme model is easier to investigate we have chosen this route in the current paper, but it might be of interest to investigate the vector meson model to see if additional phenomena can be obtained.

Acknowledgements

This work is funded by the EPSRC grant EP/K003453/1 and the STFC grant ST/J000426/1.

References

- [1] T. Sakai and S. Sugimoto, “Low energy hadron physics in holographic QCD,” *Prog. Theor. Phys.* **113** (2005) 843 [hep-th/0412141].
- [2] T. Sakai and S. Sugimoto, “More on a holographic dual of QCD,” *Prog. Theor. Phys.* **114** (2005) 1083 [hep-th/0507073].
- [3] D. K. Hong, M. Rho, H. -U. Yee and P. Yi, “Chiral Dynamics of Baryons from String Theory,” *Phys. Rev. D* **76** (2007) 061901 [hep-th/0701276 [HEP-TH]].
- [4] H. Hata, T. Sakai, S. Sugimoto and S. Yamato, “Baryons from instantons in holographic QCD,” *Prog. Theor. Phys.* **117** (2007) 1157 [hep-th/0701280 [HEP-TH]].
- [5] S. Bolognesi and P. Sutcliffe, “The Sakai-Sugimoto soliton,” arXiv:1309.1396 [hep-th].
- [6] M. Rho, S. -J. Sin and I. Zahed, “Dense QCD: A Holographic Dyonic Salt,” *Phys. Lett. B* **689** (2010) 23 [arXiv:0910.3774 [hep-th]].
- [7] V. Kaplunovsky, D. Melnikov and J. Sonnenschein, “Baryonic Popcorn,” *JHEP* **1211** (2012) 047 [arXiv:1201.1331 [hep-th]].
- [8] V. Kaplunovsky and J. Sonnenschein, “Dimension Changing Phase Transitions in Instanton Crystals,” arXiv:1304.7540 [hep-th].

- [9] B. M. A. G. Piette, B. J. Schroers and W. J. Zakrzewski, “Multi - solitons in a two-dimensional Skyrme model,” *Z. Phys. C* **65** (1995) 165 [hep-th/9406160].
- [10] W. J. Zakrzewski, *Low Dimensional Sigma Models*, Bristol, Institute of Physics Publishing, 1989.
- [11] R. A. Battye and P. M. Sutcliffe, “Skyrmions, fullerenes and rational maps,” *Rev. Math. Phys.* **14** (2002) 29 [hep-th/0103026].
- [12] F. Bruckmann, “Instanton constituents in the $O(3)$ model at finite temperature,” *Phys. Rev. Lett.* **100** (2008) 051602 [arXiv:0707.0775 [hep-th]].
- [13] M. Eto, T. Fujimori, Y. Isozumi, M. Nitta, K. Ohashi, K. Ohta and N. Sakai, “Non-Abelian vortices on cylinder: Duality between vortices and walls,” *Phys. Rev. D* **73** (2006) 085008 [hep-th/0601181].
- [14] D. Harland, “Kinks, chains, and loop groups in the CP^{n-1} sigma models,” *J. Math. Phys.* **50** (2009) 122902 [arXiv:0902.2303 [hep-th]].
- [15] D. Foster and P. Sutcliffe, “Baby Skyrmions stabilized by vector mesons,” *Phys. Rev. D* **79** (2009) 125026 [arXiv:0901.3622 [hep-th]].